Periodicals of Engineering and Natural Sciences ISSN 2303-4521
Vol. 8, No. 1, February 2020, pp.100-112

Nonlinear 3D finite element simulation of CFST columns under different confined concrete material's models

Hawra Mohamedali M.taher
Department of Civil Engineering, College of Engineering, University of Kerbala, 56001, Karbala, Iraq

ABSTRACT

Nowadays everything expands rapidly and growth with time, including the service structures to accommodate an acceptable level of service to the community. The concrete filled steel tubes is a new technique that provides some features compared with the normal concrete columns.in this study three concrete compressive stress strain models behavior have been studied to validate the adopted experimental work and find the best model that can simulate the actual data, using nonlinear finite element analysis in Abaqus. Then, three type of concrete strength where considered (C25, C40, and C60) with three Diameter of tube thickness ratios are; 165,100, and 50 for each concrete class type. Tests results have shown that the confinement effect in high strength concrete was higher than other types of concrete types, in addition to a noticeable enhancement in the ductility behavior. The adopted model was able to capture concrete compressive behavior accurately, for all curve's stages.

Keywords: 3D Finite element, CFST, Abaqus, Confined concrete coulmn

Corresponding Author:

Hawra Mohamedali M.taher
Department of Civil Engineering
College of Engineering, University of Kerbala
56001, Karbala, Iraq
E-mail: hawra.m@uokerbala.edu.iq

1. Introduction

The enhanced concrete column that externally rounded by steel tube, or the concrete filled steel column (CFST), is normally used as confinement agent to resist extra stresses generated in the concrete columns. Such technique used either to enhance an existing column strength, or could be casted as a new structural element in large span, high rise and large-scale building [1]. Due to the higher ductility, high stiffness, and higher strength relatively provided by the CFSTs, they are utilize for earthquake resistance structure or in constructing bridges piers that most of times subjected impact, dynamic loads [2, 3]. Numerous pervious and recent studied were focused on the CFST technique, with different types and shapes, such as circular, rectangular, elliptical, and square cross sections, including experimental work on their behavior subjected to pure axial and eccentric compression, tension, and torsion forces [4-8]. Also, different codes (ACI [9], AISC [10], and EC4) included design provisions for CFST columns. But only the Eurocode4 [11] presented effect of columns with steel confinement.

When CFSTs columns exposed to low magnitude forces, the steel part offers no resistance of confinement since the concrete passions ratio is lower than the steel material. Higher load results in increasing concrete longitudinal strain till failure, at such point, the concrete lateral deformation will be supported by the steel confinement part. At this time, any extra load increasement result in extra lateral deformation in concrete part, which the latter causes hoop stress for the steel tube [2, 12-15] .

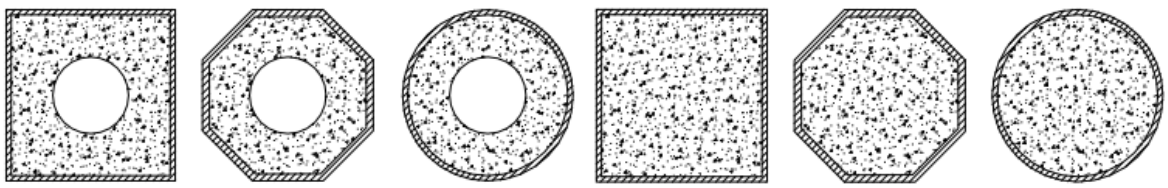

Figure 1. Common types of CFSTs [16]

The idea of confining concrete with steel tube to confine and restrain the lateral deformation behavior of concrete column has been focused by the researchers over the past 30 years [12]. Most of previous researchers approved that the CFST capacity is affected by many factors such as; length over diameter, diameter of concrete part over steel tube thickness, type of loads, and supporting conditions.
Schneider [17], investigated effect of wall thickness of different columns shapes (circular, rectangular, and square) on the nominal compressive strength capacity of short columns subjected to concentrated load. He concluded that the circular concrete column confined by steel tube offered higher confinement resistance after yielding point, higher stiffness and ductility compared with other sections.
Tokgoz and Dundar [18] investigated CFST column with normal and fiber reinforced concrete numerically. He concluded that fiber reinforced CFST had higher ductility and control crack propagation. They remarked that the steel fiber has no significant effect on the ultimate CFST capacity.
CFST behavior may influenced by many parameters, such as L/D and D/t ratios (L is length, D is core diameter, and t is wall thickness), concrete strength, and steel yield strength. considering all these effects experimentally is highly expensive and time consuming. Thus, the nonlinear finite element simulation approach may be the best solution to study and take in to account all mentioned effects [19].
This study aims to determine best available mathematical models that can accurately predict the adopted experimental work through performing 3D nonlinear finite element simulation in Abaqus and compare the results with the analytical results of the codes and standards. The study also includes further investigation of effect of concrete class and D/t ratio on the performance of CFST.

2. Prediction of confined concrete compressive stress-strain behavior introduction

In this study, three different models were investigated to predict the behavior of confined concrete strength and validate the adopted experimental work, they are; Model-1, model-2, and model-3. It worth to be mentioned that the concrete maximum strength C33 was adopted to generate the stress-strain curves of the three models, since it is the strength of the adopted experimental work, as shell be clarified in next sections.

2.1. Prediction of confined concrete compressive stress-strain behavior using Model-1

This model is adopted by Mander et al. [20]to predict stress strain behavior of CFST columns, where the curve behavior in three phases illustrated in Figure (2). the governed equations used in this model are as follows:
For the ascending part, the stress is calculated as follows:

$$\sigma_c = \frac{f_c \lambda(\varepsilon_c/\varepsilon_{co})}{\lambda - 1 + (\varepsilon_c/\varepsilon_{co})^{\lambda}} \quad (1)$$

$$\lambda = \frac{E_c}{E_c - \left(f_c/\varepsilon_{co}\right)} \quad (2)$$

$$E_c = 3320\sqrt{f_c} + 6900 \quad (3)$$

The strain at peak stress can be determined according to the concrete compressive strength as follows:

$$\varepsilon_{co} = 0.002 \; for \; f_c \leq 28MPa \quad (4)$$
$$\varepsilon_{co} = 0.003 \; for \; 28 \leq f_c < 82MPa \quad (5)$$
$$\varepsilon_{co} = 0.002 + \frac{f_c - 28}{54000} \; for \; f_c > 82MPa \quad (6)$$

For the descending parts AB, BC, and CD, the stress strain govern equation are:

$$\sigma_c = f_c \; for \; (\varepsilon_{co} < \varepsilon_c \leq 0.005) \quad (7)$$
$$\sigma_c = \beta_c . f_c \quad for \; (\varepsilon_c > 0.005) \quad (8)$$
$$\sigma_c = \beta_c . f_c + 100(0.015 - \varepsilon_c)(f_c - \beta_c . f_c) \; for \; 0.005 < \varepsilon_c \leq 0.015 \quad (9)$$

The confinement effect factor is determined as follows:

$$\beta_c = 1 for\ D/t \leq 24 \quad (10)$$
$$\beta_c = (1.5 - D/48.t) for\ 24 < D/t \leq 48 \quad (11)$$
$$\beta_c = 0.5 for\ D/t > 48 \quad (12)$$

Where:
Ec: is the concrete modulus of elasticity, MPa
D: Diameter, mm
t: tube thickness, mm
Bc: is the confinement effect factor
εc: strain at peak stress

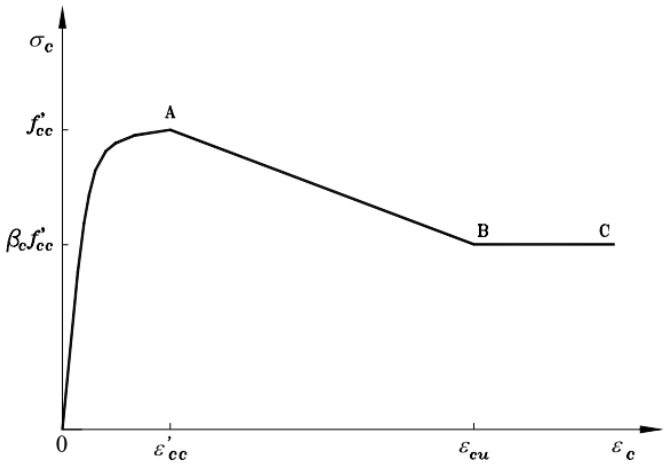

Figure 2. General stress- strain behavior of the model 1

After programming an excel sheet to predict the stress- strain behavior of confined concrete, the results of model-1 (C33) as clarified in Figure (3).
The three parts of the curves can be seen in the figure. The first phase, which no effect of steel tube confinement is exist. Followed by the second phase, which a gradual reduction in the strength with higher strain value till reaching the third phase, which continue to a fix value called the residual strength. it worth to ben mentioned that about 61% of the total concrete compressive strength was conserved.

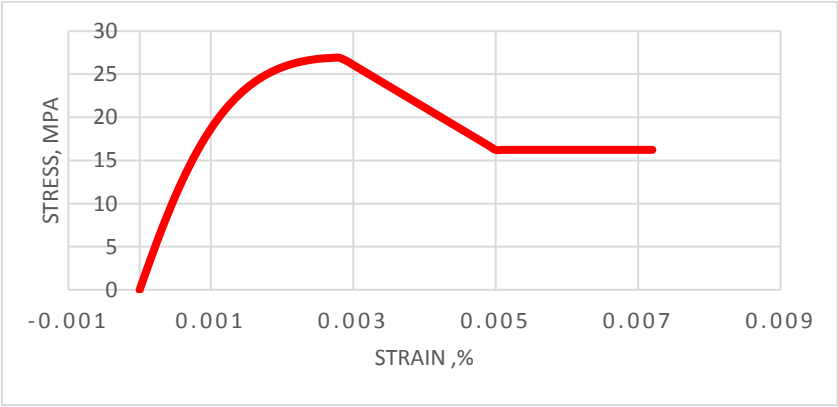

Figure 3. Results of stress- strain behavior of the model 1

2.2. Prediction of Confined concrete compressive stress-strain behavior using Model-2

This model is adopted by Liang [21] to predict stress strain behavior of CFST columns, where the curve behavior in three phases illustrated in Figure (4). the governed equations used are as follows:
For the ascending part OA, the stress is calculated from the following equation;

$$\sigma_c = \frac{f'_{cc}\lambda(\varepsilon_c/\varepsilon'_{cc})}{\lambda-1+(\varepsilon_c/\varepsilon'_{cc})^{\lambda}} \quad (13)$$

Where λ is a factor determined from the following equation:

$$\lambda = \frac{E_c}{E_c-(f'_{cc}/\varepsilon'_{cc})} \quad (14)$$

Ec is the modulus of elasticity determined from the following equation:

$$E_c = 3320\sqrt{\gamma_c f'_c} \quad (15)$$

Gamma c is a reduction factor that considers column dimensions and quality of concrete, it is determined from the following equation:

$$\gamma_c = 1.85.D_c^{-0.135}(0.85 \le \gamma_c \le 1.0) \quad (16)$$

The following factors are modifications factors which accounts for lateral confinement effect of concrete from the following equation:

$$f'_{cc} = \gamma_c f'_c + k_1 f_{rp} \quad (17)$$

$$\varepsilon'_{cc} = \varepsilon'_c(1 + k_2\frac{f_{rp}}{\gamma_c f'_c}) \quad (18)$$

The confinement pressure f_{rp} which is mainly depends on D/t ratio and material quality of steel tube is determined as follows:

$$f_{rp} = 0.7(\nu_c - \nu_s)\frac{2t}{D-2t}f_{sy} \quad for\ D/t \le 47 \quad (19)$$

$$f_{rp} = (0.006241 - 0.0000357.D/t)f_{sy} \quad for\ 47 \le D/t \le 150 \quad (20)$$

$$\nu_e = 0.2312 + 0.3582V'_e - 0.1524(\frac{f'_c}{f_{sy}}) + 4.843V'_e(\frac{f'_c}{f_{sy}}) - 9.169(\frac{f'_c}{f_{sy}})^2 \quad (21)$$

$$\nu'_e = 0.881\times10^{-6}\left(\frac{D}{t}\right)^3 - 2.58\times10^{-4}\left(\frac{D}{t}\right)^2 + 1.953\times10^{-2}\left(\frac{D}{t}\right) + 0.4011 \quad (22)$$

For parts AB,BC, and CD (as clarified in Figure()), the stresses values are determined as follows:

$$\sigma_c = \beta_c f'_{cc} + \left(\frac{\varepsilon_{cu}-\varepsilon_c}{\varepsilon_{cu}-\varepsilon'_{cc}}\right)(f'_{cc} - \beta_c f'_{cc}) \quad for \quad \varepsilon'_{cc} < \varepsilon_c \le \varepsilon_{cu} \quad (23)$$

$$\sigma_c = \beta_c f'_{cc} \quad for \quad \varepsilon_c > \varepsilon_{cu} \quad (24)$$

The confinement effect that provided by the steel tube is determined as follows:

$$\beta_c = 1.0 \quad for\frac{D}{t} \le 40 \quad (25)$$

$$\beta_c = 0.0000339\left(\frac{D}{t}\right)^2 - 0.010085\left(\frac{D}{t}\right) + 1.3491 \quad for\ 40 < \frac{D}{t} \le 150 \quad (26)$$

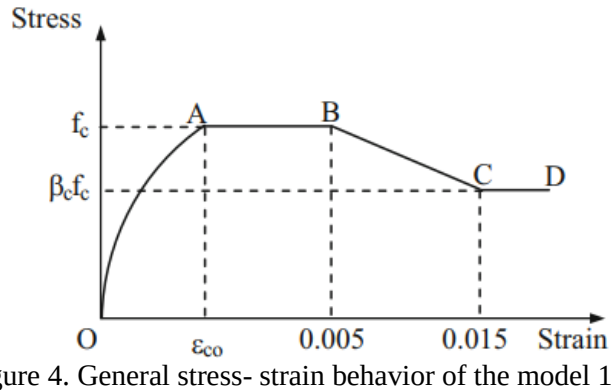

Figure 4. General stress- strain behavior of the model 1

The four parts of the curves can be seen in the figure (5). The first phase, which no effect of steel tube confinement is exist. Followed by the second phase, which is has a fix value till 0.005 strain, then reaching the third phase, which continue with linear gradual reduction till reaching the last phase, which is constant with higher strain. it worth to ben mentioned that about 50% of the total concrete compressive strength was conserved.

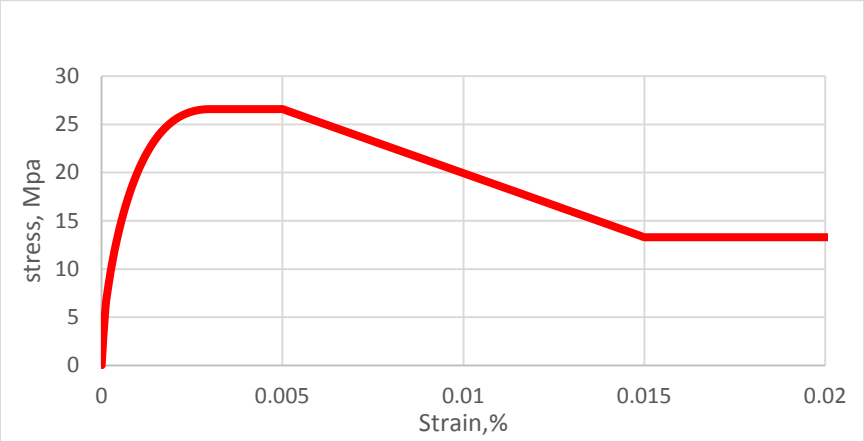

Figure 5. Results of stress- strain behavior of the model 2

2.3. Prediction of confined concrete compressive stress-strain behavior using Model-3

This model is adopted by Tao [22] to predict stress strain behavior of CFST columns, where the curve behavior in three phases illustrated in Figure (6). the governed equations used in this model are as follows:

$$\sigma = f_c \cdot \frac{A.X+B.X^2}{1+(A-2)X+(B+1)X^2} \quad (27)$$

Where:

$$X = \varepsilon/\varepsilon_{co}\,; A = \frac{E_c \varepsilon_{co}}{f_c'}; B = \frac{(A-1)^2}{0.55} - 1$$

$$\varepsilon_{co} = 0.00076 + \sqrt{(0.626 f_c' - 4.33)10^{-7}} \quad (28)$$

$$\frac{\varepsilon_{cc}}{\varepsilon_{co}} = e^k; k = (2.9224 - 0.00367 f_c') \left(\frac{f_B}{f_c'}\right)^{0.3124+0.002 f_c'} \quad (29)$$

$$f_B = \frac{(1+0.027 f_c').e^{-0.02D/t}}{1+1.6e^{-10}(f_c')^{4.8}} \quad (30)$$

$$\sigma = f_r + (f_c' - fr).\exp\left[-\left(\frac{\varepsilon-\varepsilon_{cc}}{\alpha}\right)^{\beta}\right] for \varepsilon \geq \varepsilon_{cc} \quad (31)$$

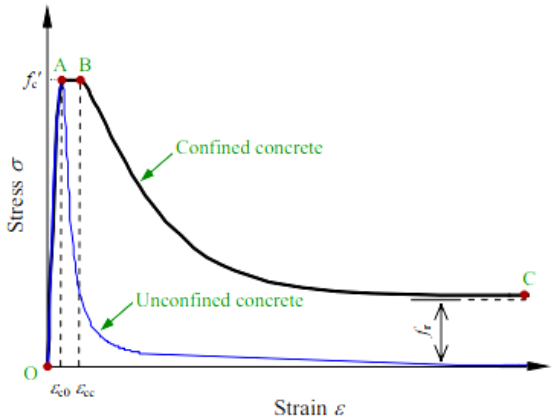

Figure 6. General stress- strain behavior of the model 3

The three parts of the curves can be seen in the Figure (7). The first phase, which no effect of steel tube confinement is exist and lock somewhat linearly behavior. Followed by the second phase, which is relatively constant with very small strain values, till reaching the third phase (the exponential part), which continue with gradual reduction in the strength with higher strain value. it worth to ben mentioned that about 41% of the total concrete compressive strength was conserved.

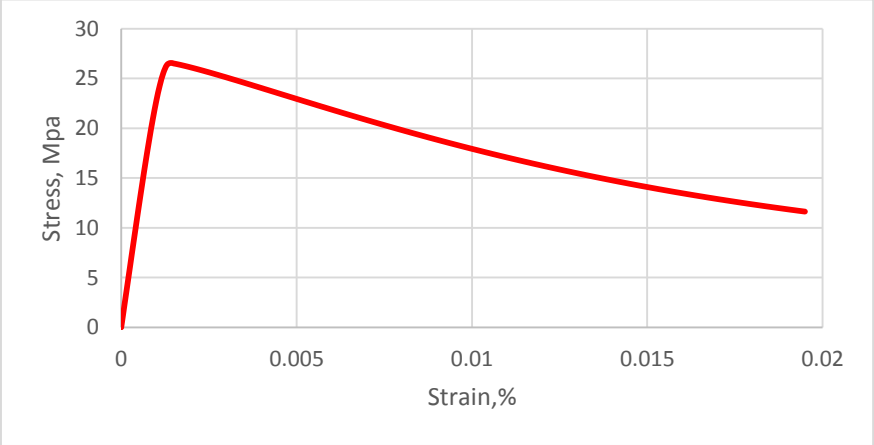

Figure 7. results of stress- strain behavior of the model 3

3. Experimental study

The study included three stages of investigations. The first stage in included prediction of confined concrete compression behavior (stress Vs strain) through investigating three various models. The second stage will include finite element simulation processes and adopting a model that will give best validity of the adopted experimental work. The results of the second stage shall be compared with ACI code and AS5100 code results in addition to the adopted experimental work result. The third stage will include further investigation through a parametric study of concrete and tube diameter over thickness ratio. Three concrete strengths shall be considered low, normal, and high strength (C25, C40, and C60), and three D/t ratios (165,100,50).

3.1. FEA Simulation

Lubliner et al [14] had predicted one of the important models that has covered by Abaqus, which is called the concrete damage plasticity model. The model then modified by Lee and Fenves [15]. The CDP model is a continuum based on the theory of plasticity which assumes tow failure criteria are, the compressive crushing and tension stiffening. In general, yield surface hardening is characterized by two main parameters are, the tensile and compressive strains. The concrete damaged plasticity model is a continuum, plasticity based, damage model for concrete behavior. The model is governed by two basic failure mechanisms, they are; compressive crushing and tensile cracking. The evolution of failure surface is governed by two major parameters are; tensile and compressive equivalent plastic strains. These two parameters are control failure mechanisms under tension and compression loadings. For concrete material, the CDP model has adopted with parameters as illustrated in Table (1). It worth to be mentioned that linear behavior of tensile stress stain curve was used in the simulation. The adopted experimental work dimensions [1] are; 165 mm,1.2 mm, and 1250 mm for Diameter, tube thickness, and length, respectively.

Table 1. CDP parameters for C33 class concrete

Property	value	CDP parameters	reference
D, mm	165	/	
t, mm	1.2	/	
Ac, mm^2	21381.83	$A_c = (\pi/4)D^2$	
As, mm^2	622.017	$A_s = \pi.D.t$	
F_{cu}, MPa	33	/	

Property	value	CDP parameters	reference
F'$_c$, MPa	26.5733	$f_c' = \left[0.76 + 0.2\log_{10}\left(\frac{f_{cu}}{19.6}\right)\right] f_{cu}$	[23]
fy, MPa	375	/	
Ec, MPa	24228.17	$E_c = 4700\sqrt{f_c'}$	[24]
Possions ratio	0.18	0.15-0.2	[11]
f_{bo}/f'_c	1.172892	$f_{bo}/f_c' = 1.5(f_c')^{-0.075}$	[25]
Kc	0.837922	$Kc = 5.5/[5 + 2(f_c')^{0.075}]$	[26]
$\boldsymbol{\xi_c}$	0.410528	$\xi_c = A_s f_y / A_c f_c'$	[27]
$\boldsymbol{\psi}$	33.18726	$\psi = 56.3(1 - \xi_c)$	[27]
$\boldsymbol{G_f}$, N/mm	0.068896	$G_f = (0.0469 d_{\max}^2 - 0.5 d_{\max} + 26)(f_c'/10)^{0.7}$	[28]
Ft, MPa	3.196057	$f_t = 0.62\sqrt{f_c'}$	[24]

a 3D deformable element, an 8-node linear brick, reduced integration, hourglass control (C3D8R), with dimensions 40mm, and total number of elements 13017, and total number of nodes are 36965 (including column neck), to reduce shear locking effect. while for steel reinforcement, a wire element 2-node linear 3-D truss (T3D2) embedded in the concrete element to simulate full bond. Figure (8) illustrates the FEA model.

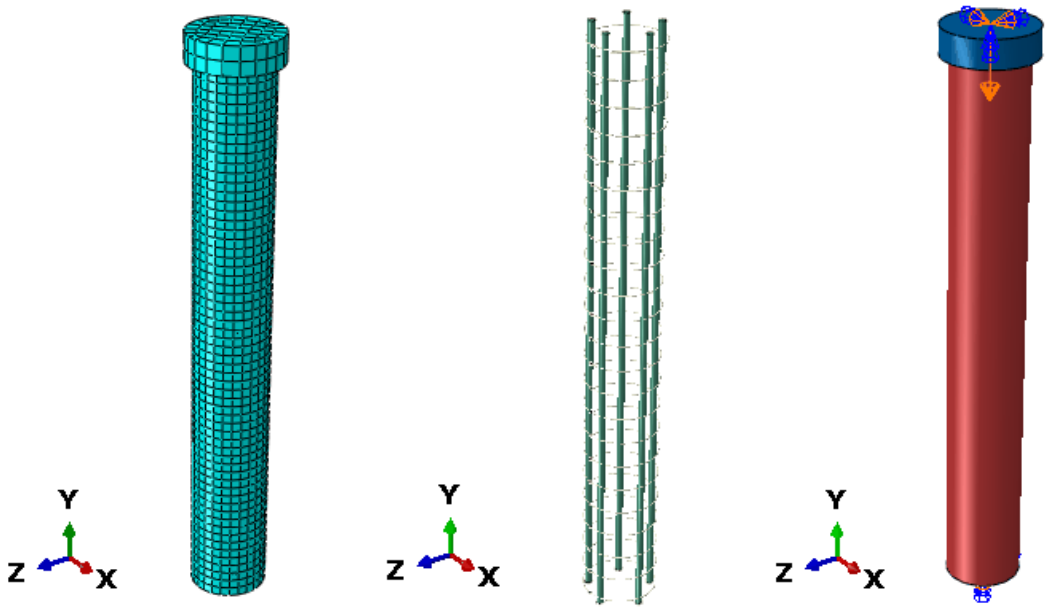

Figure 8. CFST modelling in Abaqus

The interaction between the top head and the column is normal hard contact in addition to tangential contact with 0.2 friction coefficient. The streel reinforcement was inserted inside the concrete as embedded region to simulate full interaction bond between the steel bars and the concrete. A rigid body constrain was assigned to the top head to reduce computational time and neglect stresses state in them. A quasi static load was used for the simulation, and a continuous displacement has been applied to the top of the column head till failure.

3.2. Validating the adopted model with the experimental work

After predicting the confined concrete compressive stress- strain curves, the second stage is to validate those predicted models' concrete materials using nonlinear finite element approach in Abaqus. The adopted experimental work (dimensions and materials) that will be validated are as can be seen in Figure (9) [1]. The column has 1250 mm length, 165 mm diameter, and 1.2 mm steel tube thickness. The concrete compressive strength is of class C33. The yield strength of steel tube is 375 MPa.

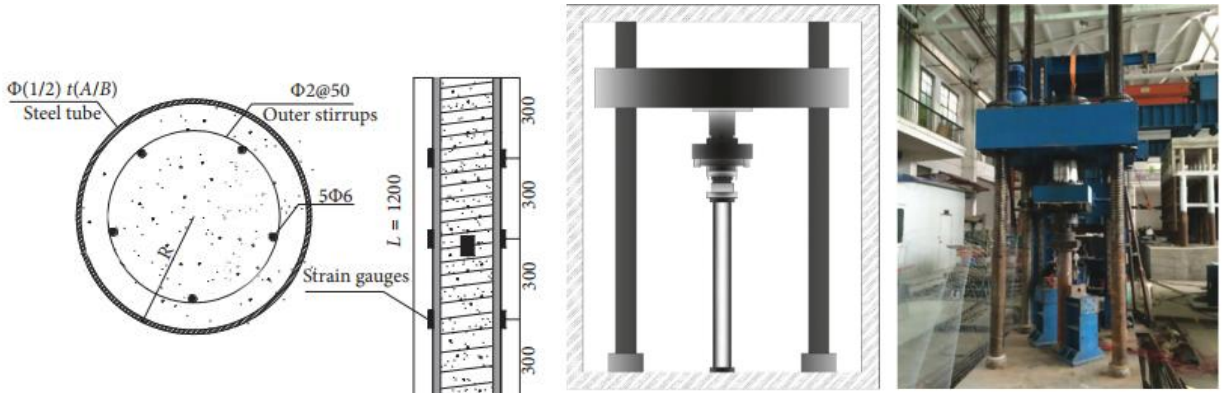

Figure 9. Test preparation and schematic view of the adopted experimental model [1]

4. Validity results and discussion

As clarified in table (2) and Figure (9), test results have shown that model-1 of concrete material reflected maximum axial pure compression force of 819 KN at 4.9 mm axial shortening. This model looks somewhat far from the experimental work, and for both values. While The concrete model material (model-2), the results have shown better results to the experimental work in term of maximum axial force, when compared relatively with the model-1. But model-2 stills reflect maximum force of 884 KN at axial shortening 5.44 mm, which still unmatched with the experimental work. The third model resulted in maximum force of 907 KN at axial shortening 8.03 mm. the last model is the best one in term of balancing both maximum axial force and axial shortening.

Figure (10), illustrates the simulated CFST strength in term of maximum axial force and maximum displacement. The study has expanded to compare the theoretical results of ACI code, AS 5100, and AISC code, as mentioned in table (2). It worth to be mentioned that the calculated values of codes results were considering the factor of safety.

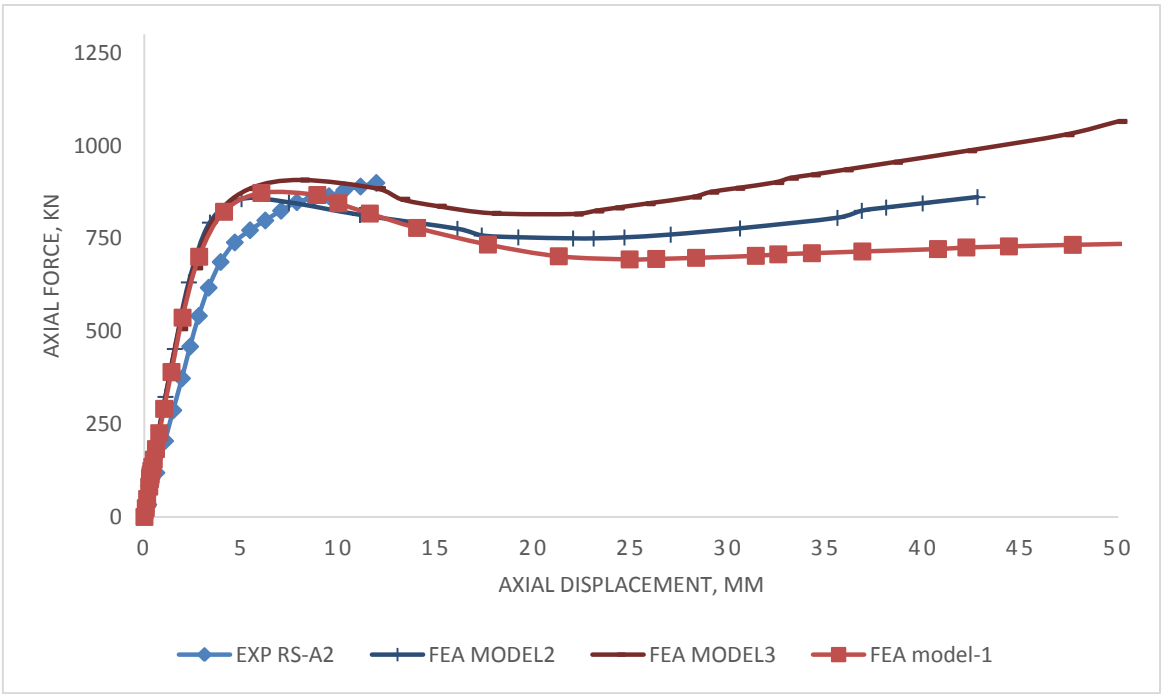

Figure 10. Validity of the adopted experimental work with various concrete composite materials

After this comprehensive comparison, model-3 of confined concrete material has been selected since it has reflected best matching compared to the experimental work. Figure (11) illustrates the results of FEA model with confined concrete material model-3. By visual inspection, the FEA results have shown similar mode of failure to the experimental model.

Table 2. Comparison of the experimental work with the FEA results and the analytical codes solution

Model type	Max axial load, KPa	Max displacement, mm
Experimental	899	11.9
Model-1	819	4.9
Model-2	884	5.44
Model-3	907	8.03
ACI	698	/
AS 5100	619	/
AISC	671	/

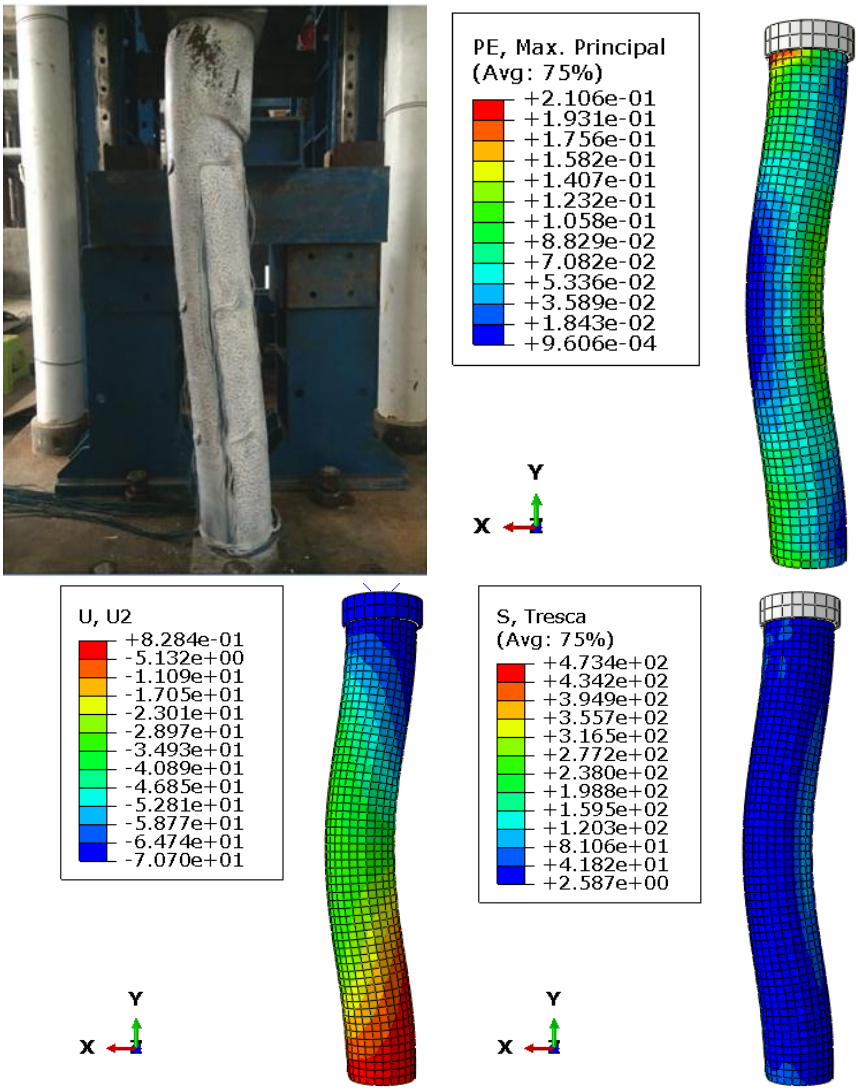

Figure 11. Comparison of the experimental work with the FEA results

4.1. Effect of concrete strength and confinement ratio (D/t) on the CFST ductility and capacity

After selecting best confined concrete model material and determination of its applicability to validate the adopted experimental work, stage 3 in this study is to study effect of concrete class strength and different diameter over tube thickness ratios. Three classes in this study were investigated, they are; C25, C40, and C60, in addition to three D/t ratio were experienced numerically in Abaqus for each concrete class type. The confined concrete stress strain for various concrete classes with various d/t ratio are illustrated in Figures (12,13, and 15).

From the previous figures, it can be observed that the ascending part for each class are the same for all D/t ratios. The d/t effect is clearly noticed in the concrete stress degradation part. Further, the confinement effect

for concrete class C25 differs from other classes. The ratio of degradation part for C25 of d/t somewhat less than other concrete classes. The concrete Class 60 have showed noticeable reduction in the strength when D/t ratio changes from 165 to 50. The same thing has been observed for concrete Class C40.

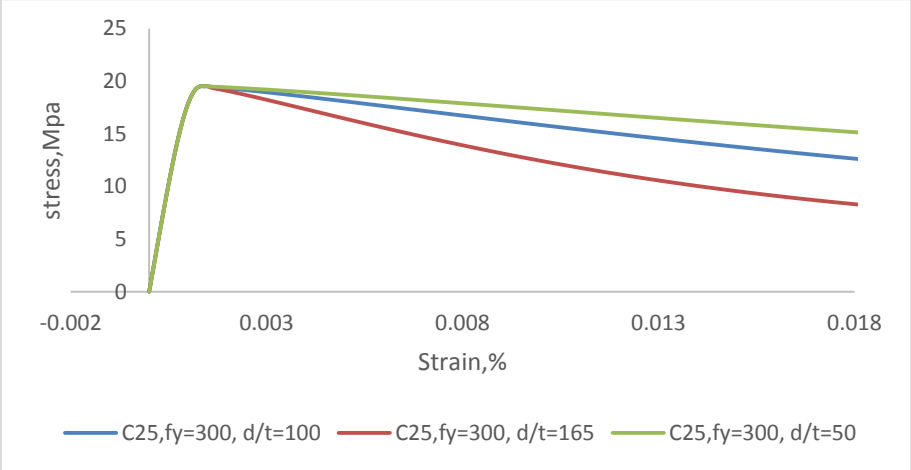

Figure 12. Results of stress- strain behavior of C25 concrete class and various D/t ratios

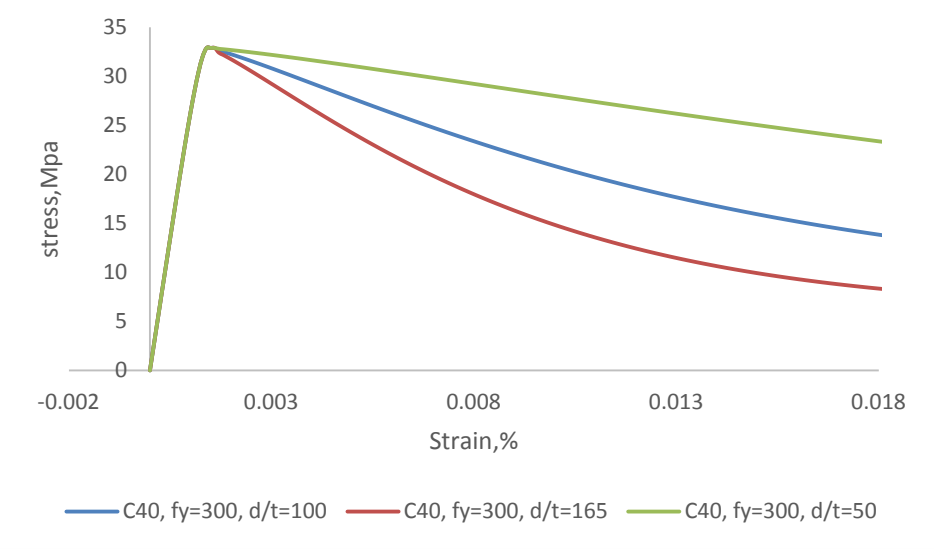

Figure 13. Results of stress- strain behavior of C40 concrete class and various D/t ratios

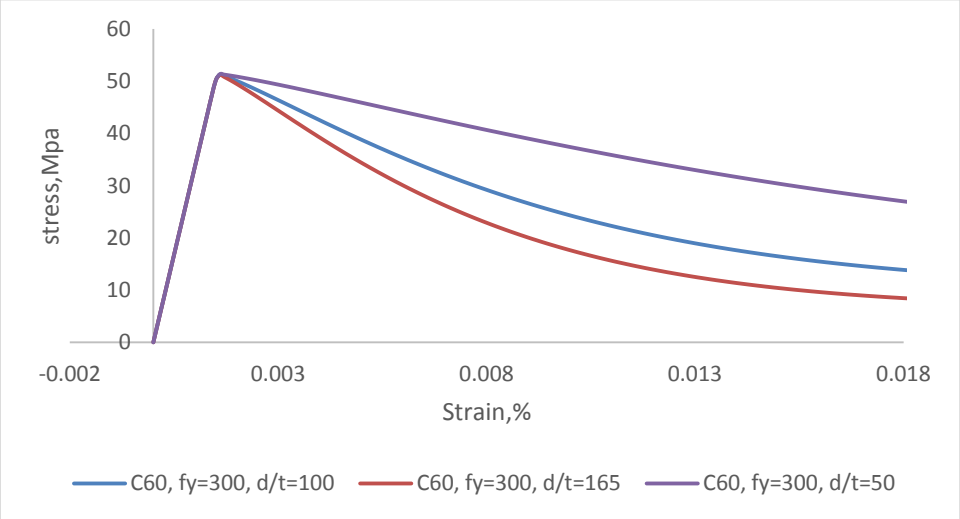

Figure 14. Results of stress- strain behavior of C60 class and various D/t ratios

Figure (13) illustrates CFST axial load capacity for different concrete classes and different D/t ratios. It can be observed that the adopted model couldn't capture the variance in the ascending part for both C25 and C40 concrete class, for all D/t ratios. While anticable change in the descending part were noticed for each class and each ratio. In the contract to concrete class C60, where both of curves load capacity parts have changed with changing D/t ratio. Also, it can be observed that the confinement effect in concrete C60 it more efficient than other concrete classes.
In the other side, the model reflected ductility of concrete class C25 higher than other classes (C40 and C60). Class 60 had less ductility among other types.

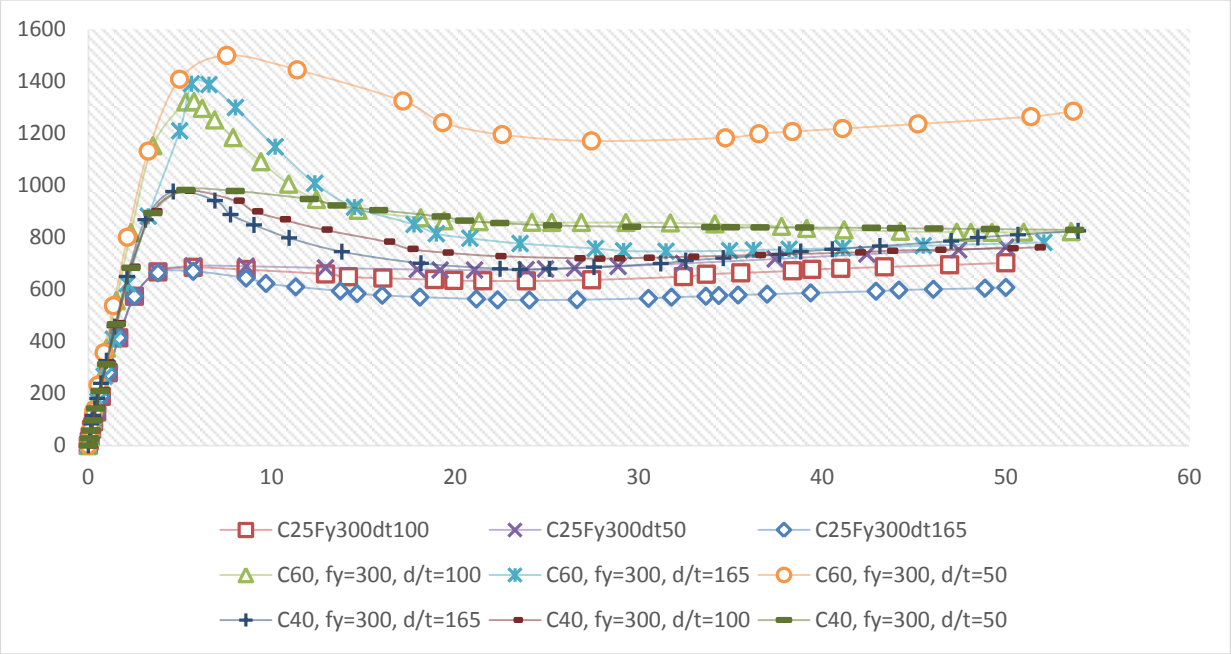

Figure 15. FEA results of model-3 for various concrete class and D/t ratios

5. Conclusions

Based on the stufdy results, the following conculsions can be drawn:

1- The adopted Model-3 reflected best validation results to the experimental work, for both criteria, maximum axial force and maximum displacement.
2- Most of the model's curves have shown that the confinement effect starts after reaching concrete maximum strain. They were having the same ascending curve.
3- The confinement effect has approved its efficiency for high strength concrete (C60), which has increased the axial load capacity about 1.55 for D/t ratio of 50, compared with and 165 ratios.
4- For normal strength concrete, the results have shown some level of enhancement in the concrete degradation behavior about 1.25 for d/t equal to 50 compared to ratio 165.
5- Low strength concrete C25 have shown an acceptable level of confinement effect in the degradation behavior part, which estimated about 1.27 for d/t ratio of 50 when compared with 165 ratio.
6- In general, confinement effect has approved its ability to enhance the maximum axial CFSTs strength, and reflected an increase of the ductility.
7- Tests results have shown that the high concrete strength CFST degradation part of the curves has higher slope than other types of CFSTs concrete strength, which is an indication of low ductility compared to others.
8- The adopted model was able to capture the variance in the descending part, in the contract to the ascending part, which all models with the same concrete compressive reflected the same behavior, except class C60.
9- The adopted model (model-3) couldn't capture effect of tube thickness increase in the maximum axial applied force. The model have should only an enhancement in the confinement effect.

References

[1] P. Li, T. Zhang, and C. Wang, "Behavior of Concrete-Filled Steel Tube Columns Subjected to Axial Compression," Advances in Materials Science and Engineering, vol. 2018, pp. 1-15, 08/26 2018.
[2] N. E. Shanmugam and B. J. J. o. c. s. r. Lakshmi, "State of the art report on steel–concrete composite columns," vol. 57, no. 10, pp. 1041-1080, 2001.
[3] E.-T. Lee, B. Yun, H. Shim, K. Chang, and G. C. J. J. o. s. e. Lee, "Torsional behavior of concrete-filled circular steel tube columns," vol. 135, no. 10, pp. 1250-1258, 2009.
[4] L.-H. Han, W. Li, and R. J. J. o. C. S. R. Bjorhovde, "Developments and advanced applications of concrete-filled steel tubular (CFST) structures: Members," vol. 100, pp. 211-228, 2014.
[5] L.-H. Han, S.-H. He, and F.-Y. J. J. o. C. S. R. Liao, "Performance and calculations of concrete filled
steel tubes (CFST) under axial tension," vol. 67, no. 11, pp. 1699-1709, 2011.
[6] Z. Ou, B. Chen, K. H. Hsieh, M. W. Halling, and P. J. J. J. o. S. E. Barr, "Experimental and analytical
investigation of concrete filled steel tubular columns," vol. 137, no. 6, pp. 635-645, 2010.
[7] T. Perea, R. T. Leon, J. F. Hajjar, and M. D. J. J. o. S. E. Denavit, "Full-scale tests of slender concrete-filled tubes: axial behavior," vol. 139, no. 7, pp. 1249-1262, 2012.
[8] L.-H. Han, H. Lu, G.-H. Yao, and F.-Y. J. J. o. C. S. R. Liao, "Further study on the flexural behaviour
of concrete-filled steel tubes," vol. 62, no. 6, pp. 554-565, 2006.
[9] A. Committee and I. O. f. Standardization, "Building code requirements for structural concrete (ACI 318-08) and commentary," 2008: American Concrete Institute.
[10] T. V. Galambos and M. J. E. J. Ravindra, AISC, "Load and resistance factor design," vol. 18, no. 3, pp. 78-84, 1981.
[11] E. C. f. S. J. p. -1-1, "Eurocode 4: Design of composite steel and concrete structures—Part 1.1: General rules and rules for buildings," ed, 2004.
[12] M. J. T.-W. S. Dundu, "Compressive strength of circular concrete filled steel tube columns," vol. 56, pp. 62-70, 2012.
[13] K. Susantha, H. Ge, and T. J. J. o. E. E. Usami, "A capacity prediction procedure for concrete-filled steel columns," vol. 5, no. 04, pp. 483-520, 2001.
[14] M. J. S. Johansson and C. Structures, "The efficiency of passive confinement in CFT columns," vol.2, no. 5, pp. 379-396, 2002.
[15] K. Sakino, H. Nakahara, S. Morino, and I. J. J. o. S. E. Nishiyama, "Behavior of centrally loaded concrete-filled steel-tube short columns," vol. 130, no. 2, pp. 180-188, 2004.
[16] M. Yu, X. Zha, J. Ye, and Y. J. E. s. Li, "A unified formulation for circle and polygon concrete-filled
steel tube columns under axial compression," vol. 49, pp. 1-10, 2013.
[17] S. P. J. J. o. s. E. Schneider, "Axially loaded concrete-filled steel tubes," vol. 124, no. 10, pp. 1125-1138, 1998.
[18] S. Tokgoz and C. J. T.-W. S. Dundar, "Experimental study on steel tubular columns in-filled with plain and steel fiber reinforced concrete," vol. 48, no. 6, pp. 414-422, 2010.
[19] Q. Q. Liang and S. J. J. o. C. S. R. Fragomeni, "Nonlinear analysis of circular concrete-filled steel tubular short columns under axial loading," vol. 65, no. 12, pp. 2186-2196, 2009.
[20] J. B. Mander, M. J. Priestley, and R. J. J. o. s. e. Park, "Theoretical stress-strain model for confined concrete," vol. 114, no. 8, pp. 1804-1826, 1988.
[21] Q. Q. J. J. o. C. S. R. Liang, "Strength and ductility of high strength concrete-filled steel tubular beam–columns," vol. 65, no. 3, pp. 687-698, 2009.
[22] Z. Tao, Z.-B. Wang, and Q. J. J. o. C. S. R. Yu, "Finite element modelling of concrete-filled steel stubcolumns under axial compression," vol. 89, pp. 121-131, 2013.
[23] Q. Yu, Z. Tao, and Y.-X. J. T.-W. S. Wu, "Experimental behaviour of high performance concrete-filled steel tubular columns," vol. 46, no. 4, pp. 362-370, 2008.
[24] A. J. A. M. Code, American Concrete Institute, Detroit, Mechigan, "Building code requirements for structural concrete and commentary," 2011.
[25] V. K. Papanikolaou, A. J. J. I. J. o. S. Kappos, and Structures, "Confinement-sensitive plasticity

constitutive model for concrete in triaxial compression," vol. 44, no. 21, pp. 7021-7048, 2007.
[26] T. Yu, J. Teng, Y. Wong, and S. J. E. S. Dong, "Finite element modeling of confined concrete-I: Drucker–Prager type plasticity model," vol. 32, no. 3, pp. 665-679, 2010.
[27] T. Yu, J. Teng, Y. Wong, and S. J. E. s. Dong, "Finite element modeling of confined concrete-II: Plastic-damage model," vol. 32, no. 3, pp. 680-691, 2010.
[28] C.-F. M. J. B. d. i. Code, "Comite euro-international du beton," vol. 213, p. 214, 1993.